Structure and Interactions of Fully Hydrated Dioleoylphosphatidylcholine Bilayers

Stephanie Tristram-Nagle,* Horia I. Petrache,# and John F. Nagle*#
*Department of Biological Sciences and #Department of Physics, Carnegie Mellon University, Pittsburgh, Pennsylvania 15213 USA

ABSTRACT This study focuses on dioleoylphosphatidylcholine (DOPC) bilayers near full hydration. Volumetric data and high-resolution synchrotron x-ray data are used in a method that compares DOPC with well determined gel phase dipalmitoylphosphatidylcholine (DPPC). The key structural quantity obtained is fully hydrated area/lipid $A_0 = 72.2 \pm 1.1$ Å^2 at 30°C, from which other quantities such as thickness of the bilayer are obtained. Data for samples over osmotic pressures from 0 to 56 atmospheres give an estimate for the area compressibility of $K_A = 188$ dyn/cm. Obtaining the continuous scattering transform and electron density profiles requires correction for liquid crystal fluctuations. Quantitation of these fluctuations opens an experimental window on the fluctuation pressure, the primary repulsive interaction near full hydration. The fluctuation pressure decays exponentially with water spacing, in agreement with analytical results for soft confinement. However, the ratio of decay length $\lambda_{fl} = 5.8$ Å to hydration pressure decay length $\lambda = 2.2$ Å is significantly larger than the value of 2 predicted by analytical theory and close to the ratio obtained in recent simulations. We also obtain the traditional osmotic pressure versus water spacing data. Our analysis of these data shows that estimates of the Hamaker parameter H and the bending modulus K_c are strongly coupled.

INTRODUCTION

One of the major goals in membrane biophysics is to obtain a reliable database for physical parameters for some of the major lipid bilayers in the biologically relevant, fluid L_α phase. These parameters include the area/lipid A and the thickness of the bilayer D_B. Such parameters are needed when discussing protein-lipid interactions and small molecule interactions with bilayers. They are also important to test and guide simulations of lipid bilayers (Feller et al., 1997; Tu et al., 1995).

Earlier, we reported our results for the dipalmitoylphosphatidylcholine (DPPC) L_α phase bilayer (Nagle et al., 1996). In the present paper, we turn our attention to the unsaturated lipid dioleoylphosphatidylcholine (DOPC). Perhaps the most complete structure of any L_α phase lipid has been obtained for DOPC (Wiener and White, 1992) at 66% relative humidity (RH). Our work on DPPC concluded that there was little change in bilayer structure with mild dehydration from fully hydrated down to 98% RH. We originally hoped that the structure would not change significantly down to 66% RH, which would thereby validate the earlier precise structure. This hope was dashed by our present study, which shows that A for DOPC is considerably different near 100% RH than that determined at 66% RH (Wiener and White, 1992), and by a recent study by Hristova and White (1998) that shows that there is a drastic change in C═C double bond distribution with dehydration past 96% RH. Therefore, there is a need to determine the bilayer structure of DOPC in the biologically relevant, fully hydrated L_α phase, which we address in this paper.

There are several methodologies for obtaining L_α phase structure. The traditional Luzzati gravimetric method is flawed for samples near full hydration because some of the water that is weighed does not go between the bilayers (Klose et al., 1988; Tristram-Nagle et al., 1993). Koenig et al. (1997) have used a combined NMR and x-ray approach to circumvent this problem. Nagle et al. (1996) used a method (McIntosh and Simon, 1986) that utilizes differences with the gel phase to obtain L_α phase results. At first, this latter method would appear to be blocked for DOPC because its main transition is below freezing (−16°C) and the low-temperature phase is not well characterized. However, the method is not restricted to different phases of the same lipid but can be extended to different lipids with the same headgroup. In this paper, we compare DOPC and DPPC and use our previous results for DPPC to obtain new results such as A for DOPC. En route, we also obtain the area compressibility K_A from the electron density profiles.

A second major goal of current research in biophysics is to characterize the fundamental interactions between macromolecules, such as DNA (Strey et al., 1997), and between multimolecular structures, such as lipid bilayers (Rand and Parsegian, 1989). At first, this might seem to be a quite different topic than the previous one of obtaining bilayer structure, but the two topics are linked in our study by methodology. Fully hydrated L_α phase bilayers are subject to strong fluctuations. These fluctuations degrade the intensities from higher orders of diffraction (Zhang et al., 1994), which complicates structural analysis. By obtaining data for the shapes of the diffraction peaks using high instrumental resolution (Zhang et al., 1996), results for the fluctuations are obtained that are then used to complete the structural analysis (Nagle et al., 1996). Although merely an interme-

Received for publication 30 March 1998 and in final form 15 May 1998.
Address reprint requests to Dr. S. Tristram-Nagle, Department of Biological Sciences, Carnegie Mellon University, Pittsburgh, PA 15213. Tel.: 412-268-3174; Fax: 412-681-0648; E-mail: stn+@andrew.cmu.edu.

0006-3495/98/08/917/09 $2.00

diate result for structural studies, the fluctuation results open a direct window on one of the important interbilayer interactions, namely, the fluctuation pressure (Petrache et al., 1998). Our data for DOPC in this paper are therefore also used to measure the fluctuation pressure. This result is then combined with osmotic pressure data as a function of water spacing, which is obtained from our structural results, and this combination leads to an improved analysis of the other interbilayer interactions for DOPC, such as hydration force and van der Waals interaction.

MATERIALS AND METHODS

Sample preparation

DOPC (1,2-dioleoyl-*sn*-glycero-3-phosphatidylcholine) was purchased from Avanti Polar Lipids (Alabaster, AL) in the lyophilized form and was used without further purification. Thin layer chromatography using chloroform/methanol/7 N NH_4OH (46:18:3, v/v) revealed only a single spot when stained with a molybdenum blue reagent (Dittmer and Lester, 1964). Polyvinylpyrrolidone (PVP) with a molecular weight of 40,000 was purchased from Aldrich Chemical Co. (Milwaukee, WI) and dried in a vacuum oven at 70°C overnight. PVP/water solutions from 0 to 60% PVP (w/w) were prepared by mixing PVP with Barnstead deionized nanopure water in 3-ml nalgene vials and allowed to equilibrate overnight at room temperature. PVP solutions were added to DOPC with nominal 3:1 (when 30% PVP in water and below) or 4:1 (when 35% PVP in water and above) weight ratio in 0.1-ml nalgene vials. The final PVP concentration in the bulk water phase was different from the initial concentration because some of the water left the polymer phase to hydrate the lipid. This effect was small, amounting to only 0.1–0.2 in the usual $\log_{10} P$ plots. However, all weight ratios were recorded to calculate the final concentrations of PVP in water. The samples were kept at room temperature for 24 h with occasional vortexing. Thin-walled 1.0-mm glass x-ray capillaries (Charles Supper Co., Natick, MA) were cleaned by sequentially washing with a chromic acid bath, deionized water, acetone, and finally copious amounts of deionized water. After drying with nitrogen, the capillaries were flame sealed at one end. Approximately 10 mg of lipid dispersion was then loaded into each capillary, and these samples were centrifuged for 10 min at 1100 × *g* in a small nalgene holder using a glycerol cushion. At PVP concentrations of 12% and above, the lipid dispersions centrifuged up instead of down at 5°C. The capillaries were then flame sealed and loaded into cassettes with 12 slots/cassette. The ends of the capillaries were embedded in a slab of silicone sealer to insure further against evaporation. The cassettes fit directly into a custom holder that was attached to X-Y-Z motorized translations to move the samples relative to the x-ray beam.

X-ray diffraction

The main x-ray source was the F3 station at the Cornell High Energy Synchrotron Source (CHESS). The CHESS beamline monochromator was used to select x-rays with $\lambda = 1.2147$ Å. An in-plane resolution of 0.002° (full-width at half maximum) in 2θ was achieved using a silicon analyzer crystal for selecting the scattered radiation. The flux at the sample was 4×10^9 photons/s in an area of 0.75 mm (vertical) × 1.0 mm (horizontal). For each peak, a coarse step scan in 2θ was taken to obtain data well into the tails of the peak and a fine step scan was taken to obtain data concentrated in the peak. D-spacing was determined from the second-order peak; no slit smear correction was necessary due to small beam size in the out-of-scattering plane direction. Normal x-ray exposures were 15–30 min, and negligible damage occurred for periods of up to an hour as assayed by observing negligible changes in the width and position of the first-order peak. Thin layer chromatography performed a month after the experiments revealed a maximum of 3% lysolecithin formation in the 10% PVP sample, but generally lysolecithin contamination was 1% or less.

The cassette was mounted so that the capillaries were positioned horizontally inside a cylindrical aluminum sample chamber with two 1.5-μm-thick Mylar windows for entry and exit of x-rays. Temperature stability was controlled to within 0.02°C by a Lake Shore Cryotronics model DRC-91C temperature controller (Westerville, OH), which responded to a 1000-ohm platinum resistance thermometer in the center of the sample cassette.

Additional *D*-spacing measurements were carried out at Carnegie Mellon University using a Rigaku fixed tube source operated at 2.3 kW. The capillaries were loaded vertically, and data were collected using a Bicron scintillation counter. Three sets of Huber slits, opened 0.7 mm horizontally and 5 mm vertically produced an in-plane resolution of 0.13° (FWHM) in 2θ. This slit configuration produced slit smear, even in the second-order peak, and a slit smear (SS) correction was made based on the correction that scales with order h as

$$D_{SS}^{h} - D_{True} = \frac{\gamma}{h^2}. \quad (1)$$

Using measurements of D_{SS} for the first two orders allows us to obtain an average value of γ from many samples. The correction for our second-order peaks was $\gamma/4 = 0.46$ Å, which was then used on the right-hand side of Eq. 1 to determine D_{True}.

Specific volume measurements

The absolute specific volume v_L of DOPC at various temperatures from 0 to 30°C was determined as described by Wiener et al. (1988), and the molecular volume $V_L = v_L M_W / N_{Avogadro}$ was obtained using a molecular weight $M_W = 786.1$.

Data fitting

X-ray diffraction data collected at CHESS were fit simultaneously for all orders using the modified Caillé theory (Zhang et al., 1994, 1996; Nagle et al., 1996). As a function of scattering angle, nearly constant backgrounds of 5 and 7 counts were obtained for water and 40% PVP solutions, respectively, compared with roughly 10,000 counts at the top of the first-order peak. Parameters determined by the fitting program were the Caillé η_1 fluctuation parameter, the mean domain size L, and the fluctuation-corrected (and Lorentz-corrected) ratios of form factors $|F_h/F_1|$.

Continuous transforms and electron density profiles

The relative continuous transform was calculated using the Shannon sampling theorem (Worthington et al., 1973), the standard phases $(--+-)$, and the ratios of form factors. The calculation uses the value of $F(0)$, which was determined using the equation (Nagle and Wiener, 1989)

$$F(0) = 2(n_L - V_L \rho_W)/A, \quad (2)$$

where $n_L = 434$ is the number of electrons in DOPC, V_L is DOPC molecular volume, $\rho_W = 0.333e/Å^3$ is the electron density of water at 30°C, and A is area/DOPC molecule. Electron density profiles were obtained from

$$\rho(z) = \rho_W + K \sum_{h=0}^{hmax} F_h \cos\left(\frac{2\pi h z}{D}\right), \quad (3)$$

where K is the instrumental scaling factor. The absolute electron density of DOPC was obtained by comparing with that of fluid phase DPPC (solid line in Fig. 6 of Nagle et al., 1996). Assuming that the volume of the phosphatidylcholine headgroup is the same in DOPC and DPPC because both are immersed in water, then the integrated electron density, above the

water level, of the two headgroup peaks in the electron density profiles should be inversely proportional to their areas A. From the area A^{DOPC} and the previous result for A^{DPPC}, the absolute scale factor K for the form factors F_h are obtained, and both the electron density profiles and the continuous transform are put on an absolute scale.

Head-to-head spacings D_{HH}

The first approximation to an important measure of the thickness of the bilayer, defined as the distance D_{HH} between headgroup peaks, is obtained from the distance between the peaks in the Fourier electron density profiles from Eq. 3. Determination of D_{HH} is subject to error due to the limited number of observable orders, although it is remarkably good when four orders of diffraction can be measured. An improved approximation (Sun et al., 1996) estimates the error by comparing the exact D_{HH} obtained from model electron density functions to D_{HH}^{4th}, which is obtained from the fourth-order Fourier reconstruction of the electron density profile for the same model. The previous application of this method (see Fig. 1 in Sun et al., 1996) used model electron density functions obtained for gel-phase DPPC bilayers (Wiener et al., 1988). For the present study, we found that the numerical corrections are very similar when model electron density functions obtained for L_α DPPC (Nagle et al., 1996, Petrache et al., 1997) are used.

Method for determination of area A

A method first employed by McIntosh and Simon (1986) for DLPE and developed by Nagle et al. (1996) for DPPC is adapted for DOPC. This method uses gel phase results, which are more extensive and complete than L_α phase results because of the extra information from wide-angle scattering, together with the measured difference between D_{HH} for the two phases and the measured volumes of both phases. This method is most inconvenient for DOPC, which only has a transition below the freezing point of water, −16°C, and no well characterized gel phase. However, the basic assumption in the method is that headgroup properties are the same in both phases, such as headgroup volume, and such an assumption is reasonable as the same headgroup is fully solvated in both phases. As DOPC and DPPC also have the same chemical headgroup, and as no assumptions are made about the hydrocarbon chains, the same method is equally applicable for obtaining A^{DOPC} by comparing DOPC to gel phase DPPC structure. Following the previous derivation (Nagle et al., 1996), the final relation for A^{DOPC} is

$$A^{DOPC} = \frac{V_L^{DOPC} - V_L^{DPPC} + A^{DPPC} D_C^{DPPC}}{D_C^{DPPC} - 1/2(D_{HH}^{DPPC} - D_{HH}^{DOPC})}. \quad (4)$$

Gel phase DPPC wide-angle results are $A^{DPPC} = 47.9$ Å^2 and $D_C^{DPPC} = 17.3$ Å (Sun et al., 1994), $V_L = 1148$ Å^3 (Nagle and Wiener, 1988), and corrected $D_{HH} = 42.8$ Å (Sun et al., 1996). As lipid volume is constant with dehydration (White et al., 1987), and as the headgroup is fully surrounded by water at the modest values of P under consideration, V_L^{DOPC} should be constant with varying P, and so only the measured D_{HH}^{DOPC} varies with P in Eq. 4.

Area compressibility modulus K_A

The basic relation for changes in area with applied osmotic pressure P is

$$A - A_0 = -A_0 D_W P / K_A, \quad (5)$$

where A_0 is the area when $P = 0$, D_W is the Luzzati water thickness under nonzero osmotic pressure P, and K_A is the area compressibility modulus. The Luzzati water thickness is given by $D_W = D - (2V_L/A)$. Equation 5 predicts that data for A versus $D_W P$ is a straight line with an intercept A_0 at $P = 0$, which determines the fully hydrated area, and a slope $-A_0/K_A$, from which K_A can be determined. We note that the Luzzati thickness is the appropriate one in Eq. 5 rather than the steric water thickness D'_W because the osmotic pressure works on all the water, which is proportional to D_W and not to D'_W.

Osmotic pressure

Osmotic pressure P was obtained from the final PVP concentration following McIntosh and Simon (1986). For reference, the highest P was 56 atm, which corresponds to 96.1% RH.

Water spacing D'_W

Water spacing was obtained by using $D'_W = D - D'_B$, where D'_B is defined (Nagle and Wiener, 1988) to be roughly the maximal thickness occupied by lipid, and D'_W therefore essentially consists only of water. This definition is basically the same as that used by McIntosh and Simon (1986) and differs from the Luzzati bilayer thickness $D_B = 2V_L/A$ used by Rand and Parsegian (1989), which imagines complete separation of water and lipid headgroup. To obtain D'_B we used $D'_B = 2D_C + 2D_H$. The thickness of the headgroup D_H was estimated from neutron diffraction (Buldt et al., 1979) to be 9.0 Å; for comparison, McIntosh has used 10 Å. The hydrocarbon thickness was obtained using $D_C = V_C/A$. Because A is not directly obtainable for low P, we used A given by the best fit to Eq. 5. The hydrocarbon volume V_C was obtained by subtracting the headgroup volume V_H from the total lipid volume V_L: $V_C = V_L - V_H$. The headgroup volume, which includes glycerols and carbonyls by definition, was previously determined to be $V_H = 319$ Å^3 (Sun et al., 1994).

RESULTS

Structure

Fig. 1 shows the absolute specific volume v_L (in ml/g) of DOPC as a function of temperature. The datum of Wiener and White (1992) is in good agreement with our data if we assume that their room temperature was 22°C. From these data the coefficient of thermal expansion for DOPC is $\alpha = 80 \pm 3 \times 10^{-5}$ deg^{-1}, similar to the average value for DMPC (Nagle and Wilkinson, 1978) above its transition, but unlike DMPC, there is apparently no temperature de-

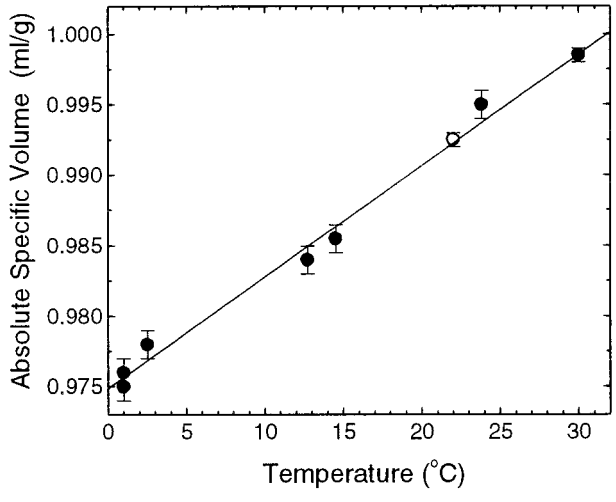

FIGURE 1 Absolute specific volumes of fully hydrated DOPC versus temperature (●). ○, datum of Wiener and White, 1992.

pendence. Using the result for v_L at 30°C, the value of V_L shown in Table 1 is obtained.

Fig. 2 shows representative data collected at CHESS. The background counts were first subtracted from all three orders. The intensities were then normalized to the peak height of the first-order peak. For easy comparison of the shapes of the peaks for the different orders, data have been plotted versus 2θ–$2\theta_h$ where $2\theta_h$ is the scattering angle of maximal intensity of the hth-order peak. The intensity is shown on a log scale to emphasize the tails. The instrumental resolution in Fig. 2 shows that the shapes of the peaks are well resolved. The Caillé η_1 parameter is obtained from the fits to the data as shown in Fig. 2. Fig. 3 shows η_1 versus D as osmotic pressure P was varied by changing the PVP concentration. As η_1 is the basic measure of fluctuations (Caillé, 1972), Fig. 3 shows that fluctuations decrease with increasing osmotic pressure and decreasing D.

Fig. 4 shows the continuous transform calculated using the phases $(--+-)$, and the four fluctuation-corrected (Nagle et al., 1996) form factors F_h (h = 1–4) obtained from the sample in 45% PVP solution. The continuous transform also uses $F(0) = 0$, which follows from Eq. 2 and V_L, assuming any reasonable estimate of A and the instrumental scaling factor K. The form factors from all samples, with one scale factor for each sample, are also shown on Fig. 4. The good agreement of F_h for other samples to the continuous transform of one sample indicates that the phases are correct and that there is no dramatic change in structure of the bilayer with increasing osmotic pressure up to 56 atm.

We were able to observe four orders of diffraction from samples of DOPC in solutions with nominally 35%, 40%, 45%, 50%, and 60% PVP. Fig. 5 shows the electron density profile for DOPC in 45% PVP solution obtained using four orders of diffraction. From the electron density profiles, D_{HH}^{4th} and the corrected D_{HH} were obtained as described in Materials and Methods, and then areas A were obtained using Eq. 4. Fig. 6 shows that areas obtained from the uncorrected D_{HH}^{4th} increase with increasing osmotic pressure,

TABLE 1 Structural results for DOPC at 30°C

	P = 0	P = 56 atm
D (Å)	63.1	49.8
v_L (ml/g)	0.9985	*
V_L (Å^3)	1303.3	*
α (deg^{-1})	0.0008	*
D_{HH} (Å)	35.3	36.4
D_C (Å)	13.6	14.3
A (Å^2)	72.2	69.0
D_B (Å)	36.1	37.3
D_W (Å)	27.0	12.5
n_W	32.5	14.5
D'_B (Å)	45.3	46.5
D'_W (Å)	17.9	3.6
n'_W	11.0	10.3
K_A (dyn/cm)	188 (113–603)	*

*Values are assumed to be the same at all P.

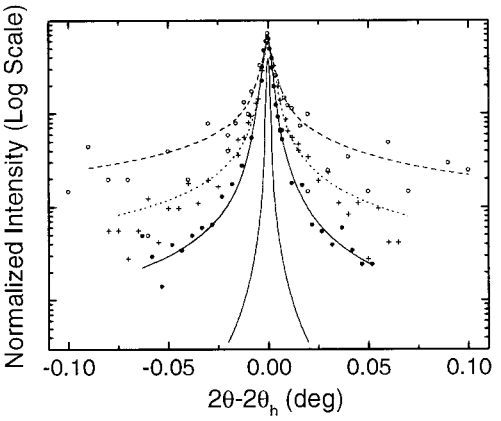

FIGURE 2 High-resolution scattering intensity data (note log scale) for DOPC in 20% PVP solution at 30°C for orders h = 1 (●), h = 2 (+), and h = 3 (○). The narrowest solid line shows the instrumental resolution. The other lines are fits to the data using modified Caillé theory (Zhang et al., 1994). For this sample, D = 55.1 Å, the Caillé η_1 = 0.037 ± 0.003, mean domain size $L = 6 \times 10^3$ Å, and χ^2 of the simultaneous fit to all orders is 1.64.

which would imply the absurd result that the compressibility modulus K_A is negative. From the results for A in Fig. 6, the fully hydrated A_0 = 72.2 ± 1.1 Å^2 was obtained from the intercept at P = 0. As explained in Materials and Methods, the slope in Fig. 6 gives the best value K_A = 188 dyn/cm; because there is considerable scatter in the data, the statistical range for K_A is quite large, from 113 to 603 dyn/cm.

Once the area is determined, a number of other structural parameters can be easily determined (Nagle and Wiener, 1988), such as the Luzzati thickness $D_B = 2V_L/A$, and the corresponding water spacing is $D_W = D - D_B$. The number of water molecules n_W is obtained using (Nagle and Wiener, 1988)

$$n_W = [(AD/2) - V_L]/V_W, \quad (6)$$

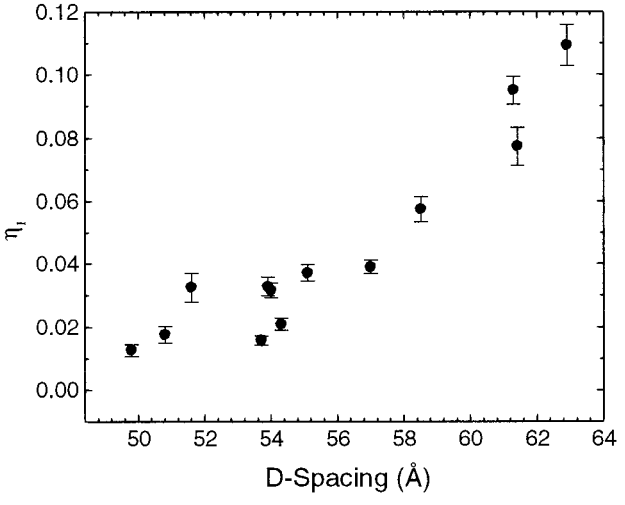

FIGURE 3 Fluctuation parameter η_1 from MCT fits versus D for DOPC at 30°C, where D is varied by applying osmotic pressure.

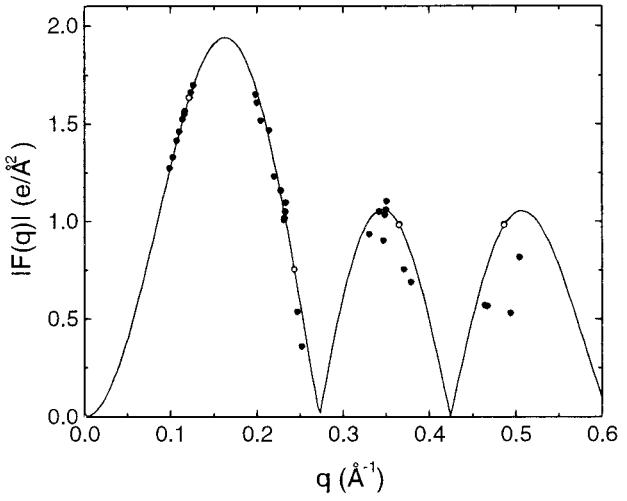

FIGURE 4 Continuous transform $|F(q)|$ in electrons/Å^2 versus q obtained using the fluctuation and Lorentz corrected form factors F_h, $h = 1$–4 (○) obtained from the sample in 45% PVP. Relative scaling factors K for the other samples are determined so as to place their F_1 on the continuous transform. Absolute scaling factors were determined as described in Materials and Methods.

where $V_W = 30.0$ Å^3 is the volume of a water molecule at 30°C. A related quantity of interest is n'_W, defined to be the number of water molecules in the headgroup region that are within the bilayer spacing D'_B; $n'_W = [(AD'_B/2) - V_L]/V_W$. Values for the various structural quantities are summarized in Table 1.

The final use of A^{DOPC} is to obtain the absolute scaling factor K for the form factors F_h, as described in Materials and Methods, so that the electron density profile in Fig. 5 and the continuous transform in Fig. 4 are placed on an absolute scale.

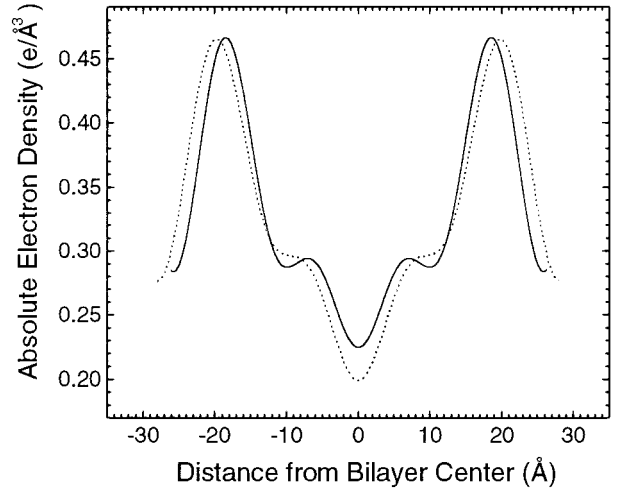

FIGURE 5 Absolute electron density profiles from fourth-order Fourier reconstructions. ———, DOPC for $P = 21.5$ atm; - - - - - -, DPPC (Fig. 6 in Nagle et al., 1996).

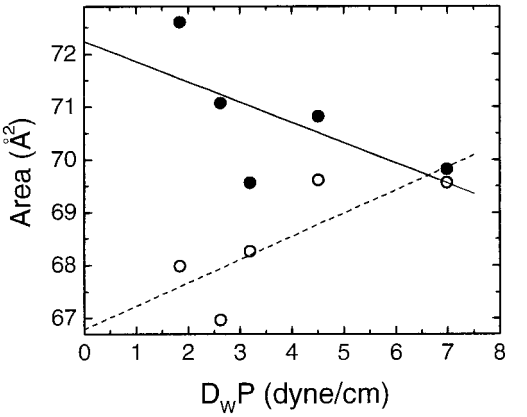

FIGURE 6 Area A versus D_WP, as described in Materials and Methods. ●, A obtained using corrected D_{HH}; ○, A obtained using uncorrected D_{HH}. The slope of the solid line is equal to $-A_0/K_A$.

Interbilayer interactions

The data for the Caillé η_1 parameter yields information about interbilayer interactions, as recently shown by Petrache et al. (1998), who derived the free energy of interaction of bilayers in a multilamellar stack:

$$F(D'_W) - F(D'_W = \infty) = V(D'_W) + \left(\frac{k_BT}{2\pi}\right)^2 \frac{1}{K_c\sigma^2}. \quad (7)$$

The $V(D'_W)$ term represents the bare free energy, which is the interaction between nonfluctuating membranes. As our data do not go to very short distances, the short-range steric interaction is not included. For uncharged lipids, the remaining bare interaction is usually considered to be the sum of the attractive van der Waals interaction and an exponential repulsion,

$$V(D'_W) = \frac{-H}{12\pi}\left(\frac{1}{D'^2_W} - \frac{2}{(D'_W + D'_B)^2} + \frac{1}{(D'_W + 2D'_B)^2}\right) + P_h\lambda e^{-D'_W/\lambda}. \quad (8)$$

(The last term in Eq. 8 is variously described as the hydration interaction (Rand and Parsegian, 1989) or a protrusion interaction (Israelachvili and Wennerstrom, 1992).) The second term in Eq. 7 is the fluctuational free energy. It involves the bending modulus K_c, of order 10^{-12} erg (Faucon et al., 1989; Evans and Rawicz, 1990; Kummrow and Helfrich, 1991), and it involves σ^2, which is the mean square fluctuation in water spacing that is obtained from the experimental determination of the Caillé order parameter using the relation $\sigma^2 = \eta_1 D^2/\pi^2$ (Petrache et al., 1998). As $P = -\partial F/\partial D'_W$, it is then natural to use the partitioning of the free energy in Eq. 7 to define a bare pressure and a fluctuation pressure,

$$P(D'_W) = P_{bare}(D'_W) + P_{fl}(D'_W). \quad (9)$$

In Fig. 7 we plot $\log \sigma^{-2}$ as a function of water spacing D'_W. The straight line represents an exponential decay in the

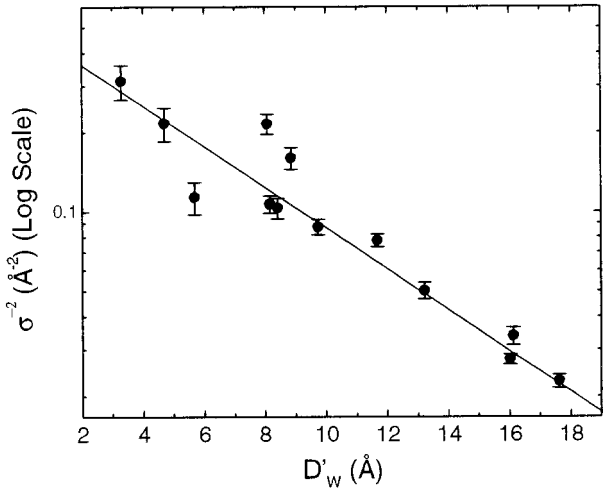

FIGURE 7 Log σ^{-2} versus D'_W from CHESS data. ———, exponential fit with decay length $\lambda_{fl} = 5.8$ Å.

fluctuation free energy, which then implies an exponential decay of the fluctuation pressure,

$$P_{fl} \sim \exp^{-D\dot{w}/\lambda_{fl}}, \tag{10}$$

with decay length λ_{fl}, the value of which is determined to be 5.8 Å for DOPC from Fig. 7.

Fig. 8 compares the fluctuation pressure to the total pressure when K_c is set to 0.7×10^{-12} erg. After subtracting P_{fl} from P, fits of Eq. 8 were then made to P_{bare}. Fig. 8 shows the best fitted hydration and van der Waals pressures. Table 2 shows results for the parameters H, P_h, and λ in Eq. 8 for fits performed for various fixed values of K_c. The fits are comparably good for all the lines in Table 2, but once K_c is chosen, the other parameters are well determined.

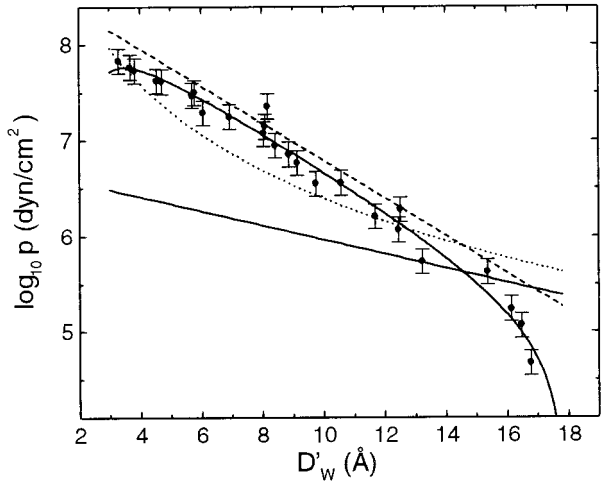

FIGURE 8 Log P versus water spacing D'_W. ●, combined data, taken at both high and low resolution. The straight solid line shows the fluctuation pressure calculated using $K_c = 0.7 \times 10^{-12}$ erg. The curved solid line shows the best fit to the data using Eq. 9. The straight dashed line shows the hydration pressure and the curved dotted line shows the van der Waals pressure obtained in this fit.

TABLE 2 Interbilayer interactions for DOPC at 30°C

K_c^*	H	P_h	λ (Å)
0.4	6.5	0.68	2.14
0.7	4.7	0.55	2.22
1.0	4.0	0.50	2.26

*Value of K_c fixed. The units for K_c are 10^{-12} erg, for H are 10^{-14} erg, and for P_h are 10^9 erg/cm^3.

DISCUSSION

Structure

The area per lipid $A_0 = 72.2$ Å^2 that we obtain for fully hydrated DOPC is considerably larger than the value 59.4 Å^2 obtained by Wiener and White (1992) at low hydration. Indeed, our value of A is so much larger than we had anticipated that it is worth emphasizing why the result must be at least qualitatively correct, by comparing with DPPC in the L_α phase. The molecular weight of DOPC (786) is greater than DPPC (734). The specific volume is very similar (only 1% larger for DPPC), so the molecular volume of DOPC (1303 Å^3) is larger than for DPPC (1232 Å^3). Nevertheless, the DOPC bilayer is thinner than the DPPC bilayer in the L_α phase, as shown in Fig. 5. This requires that A^{DOPC} be greater than $A^{DPPC} = 62.9$ Å^2 (Nagle et al., 1996), and Eq. 4 calculates by how much.

Our direct data for A are limited to samples under modest osmotic pressure P, from 10 to 56 atm. The data, shown in Fig. 6, are clearly rather scattered from the straight line that is required for an elastic compressibility modulus. Nevertheless, these data suffice to obtain a reasonably precise extrapolation to a fully hydrated area $A_0 = 72.2 \pm 1.1$ Å^2. The scatter in the data makes it much more difficult to obtain a precise value for K_A, and we obtain a range of 113–603 dyn/cm, with a best value of 188 dyn/cm. However, the data in Fig. 6 and the continuous scattering transforms in Fig. 4 are consistent with no drastic phase transition taking place in this range of P, so the data should obey an elastic theory, and therefore straight line extrapolation to A_0 in Fig. 6 is a valid procedure. This conclusion is supported by the recent results of Hristova and White (1998) who reported that the double bond distribution changed very little in this same range of P (using 30–60% PVP solutions).

Hristova and White (1998) also reported that substantial changes take place at P only slightly higher than our maximal P, which indicates that trying to obtain more precise values of K_A for DOPC by extending the pressure range would not be successful. In this context, it is of interest to calculate $K_A^{apparent}$ using Eq. 5, our $A_0 = 72.2$ Å^2, $P = 570$ atm for 66% RH, $D_W = 2.7$ Å from $n_W = 5.3$ waters/lipid, and $A = 59.4$ Å^2 from Wiener and White (1992). This calculation yields $K_A^{apparent} = 87$ dyn/cm. The result of Hristova and White (1998) that some kind of transition takes place between our highest pressure $P = 56$ atm and $P = 570$ atm is consistent with having $K_A^{apparent}$ smaller than our best value $K_A = 188$ dyn/cm for the true elastic modulus.

Our value of A_0 for DOPC may be compared with literature values. Rand and Parsegian (1989) reported $A_0 = 72.1$ Å^2 after reworking earlier data using an estimated compressibility $K_A = 145$ dyn/cm. This is much better agreement with our A_0 than for DPPC where their method gives $A_0 = 68.1$ Å^2, which is larger than the value $A_0 = 62.9$ Å^2 that was obtained (Nagle et al., 1996) by the same methods employed in this paper. The earlier data (Lis et al., 1982) gave $A_0 = 82$ Å^2 for DOPC using the unadulterated Luzzati method, which is now recognized as giving values of A_0 that are too large (Tristram-Nagle et al., 1993; Koenig et al., 1997; Gawrisch et al., 1985). However, Gruner et al. (1988) also used the Luzzati method and obtained $A_0 = 70$ Å^2, but at the much lower temperature of 2°C. Again at low temperatures, from calorimetry of the ice transition, it has been reported (Ulrich et al., 1994) that the number of waters/lipid n_w is 20; using Eq. 6 and $n_w = 20$ gives $A_0 = 62$ Å^2 at 30°C, which is clearly too small. However, these two low-temperature results could be consistent with each other as the Luzzati method overestimates A_0, and they could be consistent with our result at 30°C if there is a strong temperature dependence in A_0 and n_w for DOPC. This suggests that future studies of DOPC as a function of temperature could be interesting.

There are no literature values for area compressibility for DOPC to compare with our best value $K_A = 188$. (The value $K_A = 145$ dyn/cm suggested in Table 1 of Rand and Parsegian (1989) was inferred from DMPC.) Considering other phosphatidylcholine lipids, Koenig et al. (1997) give $K_A = 136$ (123–152) dyn/cm for DMPC and $K_A = 210 \pm 10$ dyn/cm for DOPC for compression. For the same lipids under tension, Evans and Needham (1987) give $K_A = 144.9 \pm 10.5$ and $K_A = 199.6 \pm 12.7$, respectively. Although our K_A for DOPC is not so precise, our best value is consistent with the intuition that K_A should increase with chain length and decrease with number of unsaturated C=C bonds. We also note that changes in A^F_{DPPC} with osmotic pressure were not directly observed by Nagle et al. (1996) because P went up to only 23 atm instead of the 56 atm in this paper. In retrospect, the result, that A^F_{DPPC} obtained using the Fourier method near $P = 23$ atm was lower than A^F_{DPPC} obtained using a model method that employed the data at all P, is qualitatively consistent with having a finite compressibility K_A in DPPC. The present paper goes beyond the earlier paper (Nagle et al., 1996) in that we have obtained a rough estimate of K_A for DOPC whereas K_A for DPPC has yet to be measured.

We emphasize that obtaining values of A_0 that are consistent with the correct sign of K_A requires correcting the head-to-head spacing D_{HH} obtained at low spatial resolution with small numbers of x-ray reflections. Four orders of reflection allow a quite good estimate of D_{HH}, but this estimate is systematically biased as D_{HH}/D varies with dehydration. Electron density models have been used to estimate the correction (Sun et al., 1996). We have used models where the headgroup electron density profile is represented by one Gaussian peak because this is close to the resolution of our data. More refined electron density models, such as two Gaussians in the headgroup region (Wiener et al., 1989) should be used to estimate the correction if more orders of diffraction are obtained. It may be noted that the corrections to D_{HH} range from 1.9 Å at $P = 10$ atm to 0.2 Å at $P = 56$ atm.

Our primary structural results, summarized in Table 1, rely upon the collection of x-ray scattering data at very high instrumental resolution. As shown in Fig. 2, the power law tails in the scattering data increase with diffraction order and the scattering line shapes can be analyzed as the resolution peak has a smaller width, 0.002° in 2θ, than the x-ray scattering peaks. These tails result from fluctuations in the multilamellar samples (Smith et al., 1987; Zhang et al., 1996). This causes loss of intensity under the higher-order peaks, requiring a correction to obtain the full intensity. The modified Caillé theory for this correction has been worked out for powder samples (Zhang et al., 1994) and has been used to determine the structure of fluid or L_α phase DPPC (Nagle et al., 1996) and DMPC and egg PC (Petrache et al., 1998).

Interbilayer interactions

Besides being a complicated necessity for obtaining structural results, the scattering line shapes give direct information about one of the important interbilayer interactions, namely, the fluctuation pressure. This pressure is a very important factor that affects the fully hydrated water spacing D'_W and the concomitant D spacing. The studies of McIntosh and Simon (1993) concluded that the major reason for the larger water spacing D'_W in flexible L_α lipid compared with rigid gel or subgel lipid is the much smaller fluctuation pressure in the latter phases. We think this is a valid conclusion, but obtaining this conclusion involved deconvolving one set of data, osmotic pressure P versus D'_W, into three different pressures: one due to hydration forces P_h, one due to van der Waals interactions P_{vdW}, and finally the fluctuation pressure P_{fl} (McIntosh and Simon, 1993). Our innovation is to obtain independent experimental results for the fluctuation pressure.

One issue regarding the fluctuation pressure is its functional dependence on D'_W. The original Helfrich (1978) theory gave a $1/D'^2_W$ dependence, but this was for hard confinement with no soft interactions, such as hydration or van der Waals forces. Analytical theories of soft confinement (Evans and Parsegian, 1983; Podgornik and Parsegian, 1992) give an exponential dependence $P_{fl} = C \exp(-D'_W/\lambda_{fl})$ where $\lambda_{fl} = 2\lambda$ was predicted to be twice the decay length λ of the hydration force. Our data in Fig. 7 are indeed consistent with an exponential decay, but we find that λ_{fl} is significantly greater than 2λ, not only for DOPC in this paper but also for DMPC, DPPC, and EPC (Petrache et al., 1998). Simulations of interacting bilayers (Gouliaev and Nagle, 1998) also obtain the same inequality. It therefore appears that the theory of soft confinement is on the right

track, but that improvements, such as Monte Carlo simulations, are needed.

After obtaining the functional form of P_{fl} we investigated the values of the fundamental parameters for interbilayer interactions by fitting to the osmotic pressure data. The only anomalous aspect of the fit shown in Fig. 8 occurs in the limit as D'_W approaches zero. Because of the singularity in the van der Waals interaction, the fitting model formally predicts that the negative van der Waals pressure exceeds the hydration pressure, which would lead to a negative total pressure for smaller D'_W than shown in Fig. 8. This is an artifact of the model that disappears if the steric interactions discussed by McIntosh et al. (1987) are considered. As our data did not extend far into this regime, we did not add a steric pressure to the model because it would have been poorly determined. However, to determine whether our fits were sensitive to this artifact, we also performed the fits with the three data points at highest pressure removed and found little difference in the fitted parameters, so we believe this is not a concern for our data. Indeed, we suggest that having more data at higher P would require adding another pressure to the model and would not help to determine the parameters that are most relevant for fully hydrated bilayers.

Our fits did not lead to well determined values for the entire set of parameters. However, if the value of either K_c or H is assumed, then the other parameters are well determined. Specifically, this means that all of the parameter sets shown in Table 2 are possible. Therefore, at least one additional datum is required to complete the task of evaluating the significant parameters for the interbilayer interactions. Obtaining K_c or H independently is not easy, and we are unaware of quantitatively reliable results for DOPC. However, the range of K_c for various lipids is 0.5×10^{-12} to 2×10^{-12} erg (Evans and Rawicz, 1990; Faucon et al., 1989; Kummrow and Helfrich, 1991), and H about approximately 4×10^{-14} to 5×10^{-14} erg has been proposed (Parsegian, 1993). The latter value of H favors line 2 in Table 2 and a value of $K_c \sim 0.7 \times 10^{-12}$ erg. The parameters in Table 2 are in the same range as our recent results for three other phosphatidylcholines: EPC, DMPC, and DPPC, all in the fluid phase (Petrache et al., 1998). There are only small differences in our best values for the hydration decay length λ, which is closer to 2 Å for the other lipids, and for those lipids, P_h was closer to 1.0×10^9 erg/cm^3. Apart from the fact that P_h is very sensitive to the choice of D'_B, the lower value of P_h and the larger value of λ may be related to the larger area per molecule in the case of DOPC. We conclude that, although our analysis does not allow us to obtain all the information one would like about interbilayer interactions, these fluctuation data do narrow the ranges of possible values.

We acknowledge Prof. R. M. Suter for configuring the high-resolution x-ray setup at CHESS and Tom Whittaker for help with the sample preparations and preliminary data collection at CMU. We thank Drs. S. H. White and K. Hristova for sending us their results before publication. We thank our CHESS collaborator Dr. R. L. Headrick and the staff at CHESS and we acknowledge CHESS for beamtime under proposal P727.

This research was supported by National Institutes of Health grant GM44976.

REFERENCES

Buldt, G., H. U. Gally, J. Seelig, and G. Zaccai. 1979. Neutron diffraction studies on phosphatidylcholine model membranes. I. Head group conformation. *J. Mol. Biol.* 134:673–691.

Caillé, A. 1972. Physique cristalline: remarques sur la diffusion des rayons X dans les smectiques. *A.C.R. Acad. Sci. Paris Ser. B.* 274:891–893.

Dittmer, J. C., and R. L. Lester. 1964. A simple, specific spray for the detection of phospholipids on thin-layer chromatograms. *J. Lipid Res.* 5:126–127.

Evans, E. A., and V. A. Parsegian. 1983. Energetics of membrane deformation and adhesion in cell and vesicle aggregation. *Ann. N.Y. Acad. Sci.* 416:13–33.

Evans, E. A., and D. Needham. 1987. Physical properties of surfactant bilayer membranes: thermal transitions, elasticity, rigidity, cohesion and colloidal interactions. *J. Phys. Chem.* 91:4219.

Evans, E. A., and W. Rawicz. 1990. Entropy-driven tension and bending elasticity in condensed-fluid membranes. *Phys. Rev. Lett.* 64:2094.

Faucon, J. F., M. D. Mitov, P. Méléard, I. Bivas, and P. Bothorel. 1989. Bending elasticity and thermal fluctuations of lipid membranes: theoretical and experimental requirements. *J. Phys. France.* 50:2389.

Feller, S. E., R. M. Venable, and R. W. Pastor. 1997. Computer simulation of a DPPC phospholipid bilayer: structural changes as a function of molecular surface area. *Langmuir.* 13:6555–6561.

Gawrisch, K., W. Richter, A. Mops, P. Balgavy, K. Arnold, and G. Klose. 1985. The influence of water concentration on the structure of egg yolk phospholipid/water dispersions. *Studia Biophys.* 108:5–16.

Gouliaev, N., and J. F. Nagle. 1998. Simulations of a single membrane between two walls using a new Monte Carlo method. *Phys. Rev. E.* In press.

Gruner, S. M., M. W. Tate, G. L. Kirk, P. T. C. So, D. C. Turner, D. T. Keane, C. P. S. Tilcock, and P. R. Cullis. 1988. X-ray diffraction study of polymorphic behavior of N-methylated DOPE. *Biochemistry.* 27: 2853–2866.

Helfrich, W. 1978. Steric interaction of fluid membranes in multilayer systems. *Z. Naturforsch.* 33a:305–315.

Hristova, K., and S. H. White. 1998. Determination of the hydrocarbon core structure of fluid dioleoylphosphocholine (DOPC) bilayers by x-ray diffraction using specific bromination of the double-bonds: effect of hydration. *Biophys. J.* 74:2419–2433.

Israelachvili, J. N., and H. Wennerstrom. 1992. Eutropic forces between amphiphilic surfaces in liquids. *J. Phys. Chem.* 96:520–531.

Klose, G., B. Konig, H. W. Meyer, G. Schulze, and G. Degovics. 1988. Small-angle x-ray scattering and electron microscopy of crude dispersions of swelling lipids and the influence of the morphology on the repeat distance. *Chem. Phys. Lipids.* 47:225–234.

Koenig, W., H. H. Strey, and K. Gawrisch. 1997. Membrane lateral compressibility determined by NMR and x-ray diffraction: effect of acyl chain polyunsaturation. *Biophys. J.* 73:1954–66.

Kummrow, M., and W. Helfrich. 1991. Deformation of giant lipid vesicles by electric fields. *Phys. Rev. A.* 44:8356–8360.

Lis, L. J., M. McAlister, N. L. Fuller, R. P. Rand, and V. A. Parsegian. 1982. Interactions between neutral phospholipid bilayer membranes. *Biophys. J.* 37:657–666.

McIntosh, T. J., and S. Simon. 1986. Area per molecule and distribution of water in fully hydrated dilaurylphosphatidylethanolamine bilayers. *Biochemistry.* 25:4948–4952.

McIntosh, T. J., and S. Simon. 1993. Contributions of hydration and steric (entropic) pressure to the interactions between phosphatidylcholine bilayers: experiments with the subgel phase. *Biochemistry.* 32: 8374–8384.

McIntosh, T. J., A. D. Magid, and S. A. Simon. 1987. Steric repulsion between phosphatidylcholine bilayers. *Biochemistry.* 26:7325.

Nagle, J. F., and M. C. Wiener. 1988. Structure of fully hydrated dispersions. *Biochim. Biophys. Acta.* 942:1–10.

Nagle, J. F., and M. C. Wiener. 1989. Relations for lipid bilayers: connections of electron density profiles to other structural quantities. *Mol. Cryst. Liq. Cryst.* 144:235–255.

Nagle, J. F., and D. A. Wilkinson. 1978. Lecithin bilayers: density measurements and molecular interactions. *Biophys. J.* 23:159–175.

Nagle, J. F., R. Zhang, S. Tristram-Nagle, W-S. Sun, H. I. Petrache, and R. M. Suter. 1996. X-ray structure determination of fully hydrated L_α phase dipalmitoylphosphatidylcholine bilayers. *Biophys. J.* 70: 1419–1431.

Parsegian, V. A. 1993. Reconciliation of van der Waals force measurements between phosphatidylcholine bilayers in water and between bilayer-coated mica surfaces. *Langmuir.* 9:3625–3628.

Petrache, H. I., S. E. Feller, and J. F. Nagle. 1997. Determination of component volumes of lipid bilayers from simulations. *Biophys. J.* 70: 2237–2242.

Petrache, H. I., N. Gouliaev, S. Tristram-Nagle, R. Zhang, R. M. Suter, and J. F. Nagle. 1998. Interbilayer interactions from high resolution x-ray scattering. *Phys. Rev. E.* 57:7014–7024.

Podgornik, R., and V. A. Parsegian. 1992. Thermal-mechanical fluctuations of fluid membranes in confined geometries: the case of soft confinement. *Langmuir.* 8:557–562.

Rand, P. R., and V. A. Parsegian. 1989. Hydration forces between phospholipid bilayers. *Biochim. Biophys. Acta.* 988:351–376.

Smith, G. S., C. R. Safinya, D. Roux, and N. A. Clark. 1987. X-ray study of freely suspended films of a multilamellar lipid system. *Mol. Cryst. Liq. Cryst.* 144:235–255.

Strey, H. H., V. A. Parsegian, and R. Podgornik. 1997. Equation of state for DNA liquid crystals: fluctuation enhanced electrostatic repulsion. *Phys. Rev. Lett.* 78:895–898.

Sun, W.-J., R. M. Suter, M. A. Knewtson, C. R. Worthington, S. Tristram-Nagle, R. Zhang, and J. F. Nagle. 1994. Order and disorder in fully hydrated unoriented bilayers of gel phase dipalmitoylphosphatidylcholine. *Phys. Rev. E.* 49:4665–4676.

Sun, W.-J., S. Tristram-Nagle, R. M. Suter, and J. F. Nagle. 1996. Structure of gel phase saturated lecithin bilayers: temperature and chain length dependence. *Biophys. J.* 71:885–891.

Tristram-Nagle, S., R. Zhang, R. M. Suter, C. R. Worthington, W.-J. Sun, and J. F. Nagle. 1993. Measurement of chain tilt angle in fully hydrated bilayers of gel phase lecithins. *Biophys. J.* 64:1097–1109.

Tu, K., D. J. Tobias, and M. L. Klein. 1995. Constant pressure and temperature molecular dynamics simulation of a fully hydrated liquid crystal phase dipalmitoylphosphatidylcholine bilayer. *Biophys. J.* 69: 2558–2562.

Ulrich, A. S., M. Sami, and A. Watts. 1994. Hydration of DOPC bilayers by differential scanning calorimetry. *Biochim. Biophys. Acta.* 1191: 225–230.

White, S. H., Jacobs, R. E., and King, G. I. 1987. Partial specific volumes of lipid and water in mixtures of egg lecithin and water. *Biophys. J.* 52:663–665.

Wiener, M. C., R. M. Suter, and J. F. Nagle. 1989. Structure of fully hydrated gel phase of dipalmitoylphosphatidylcholine. *Biophys. J.* 55: 315–325.

Wiener, M. C., S. Tristram-Nagle, D. A. Wilkinson, L. E. Campbell, and J. F. Nagle. 1988. Specific volumes of lipids in fully hydrated bilayer dispersions. *Biochim. Biophys. Acta.* 938:135–142.

Wiener, M. C., and S. H. White. 1992. Structure of a fluid dioleoylphosphatidylcholine bilayer determined by joint refinement of x-ray and neutron diffraction data. II. Distribution and packing of terminal methyl groups in a fluid lipid bilayer. *Biophys. J.* 61:428–433.

Worthington, C. R., G. I. King, and T. J. McIntosh. 1973. Direct structure determination of multilayered membrane-type systems which contain fluid layers. *Biophys. J.* 13:480–494.

Zhang, R., R. M. Suter, and J. F. Nagle. 1994. Theory of the structure factor of lipid bilayers. *Phys. Rev. E.* 50:5047–5060.

Zhang, R., S. Tristram-Nagle, W. Sun, R. L. Headrick, T. C. Irving, R. M. Suter, and J. F. Nagle. 1996. Small-angle x-ray scattering from lipid bilayers is well described by modified Caillé theory but not by paracrystalline theory. *Biophys. J.* 70:349–357.